POST-PRINT VERSION

February 2021

Optimization-Based Methodology for Selection of a Pump-as-Turbine in Water Distribution Networks: Effects of Different Objectives & Machine Operation Limits on Best Efficiency Point.

Djordje Mitrovic

Jorge García Morillo

Juan Antonio Rodríguez Díaz

Aonghus Mc Nabola

Paper accepted to be published in

Journal of Water Resources Planning and Management

Editorial: ASCE, ISSN: 0733-9496

http://dx.doi.org/10.1061/(ASCE)WR.1943-5452.0001356

Mitrovic, D., Morillo, J.G., Rodríguez Díaz, J.A., Mc Nabola, A., 2021. "Optimization-Based Methodology for Selection of Pump-as-Turbine in Water Distribution Networks: Effects of Different Objectives and Machine Operation Limits on Best Efficiency Point". *J. Water Resour. Plan. Manag.* 147(5): 1:16

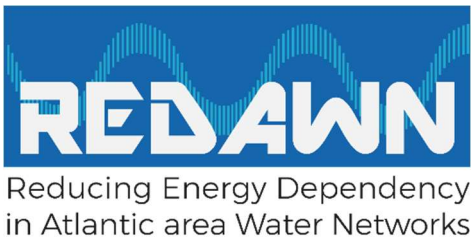

Optimization-Based Methodology for Selection of a Pump-as-Turbine in Water Distribution Networks: Effects of Different Objectives & Machine Operation Limits on Best Efficiency Point.

Djordje Mitrovic[1*], Jorge García Morillo[2], Juan Antonio Rodríguez Díaz[3] and Aonghus Mc Nabola[4]

[1] Ph.D. student, Department of Civil, Structural & Environmental Engineering, Trinity College Dublin, College Green, Dublin 2, Dublin, Ireland. Email: mitrovid@tcd.ie

[2] Professor, Department of Agronomy, University of Córdoba, International Campus of Excellence ceiA3, 14071 Córdoba, Spain. Email: jgmorillo@uco.es;

[3] Professor, Department of Agronomy, University of Córdoba, International Campus of Excellence ceiA3, 14071 Córdoba, Spain. Email: jarodriguez@uco.es;

[4] Professor, Department of Civil, Structural & Environmental Engineering, Trinity College Dublin, College Green, Dublin 2, Dublin, Ireland. amcnabol@tcd.ie.

*****Corresponding Author Email: mitrovid@tcd.ie;

Abstract

In recent years, many researchers recognized pressure reducing valves (PRVs) as potential micro-hydropower sites, aiming to improve the efficiency of the water networks. Pump as Turbines (PATs) have been pointed out as the most suitable technology because of their favourable cost. Most of the methodologies available in the literature for selection of a PAT to replace a PRV follow a traditional approach that is based on scaling a prototype data using the affinity curves, thus restricting the solution space only to these curves. The optimization based methodology presented in this paper employs the classical hydraulic regulation scheme with the Nedler-Mead simplex direct search algorithm to search for the optimal solution within space that is constrained only by the boundaries of available centrifugal PATs on the market. The methodology also defines the PAT's operation limits based on the PAT's relative mechanical power. Improvements gained by using the novel methodology have been demonstrated on real-world case studies from Ireland and Italy that were previously used in the literature. The results of the considered sites also suggest that the maximal global plant's efficiency is around 80% of the maximal efficiency of the theoretically optimal PAT. The paper also examines effects of different objective functions and different PAT's operation limits on the selection of the optimal PAT.

Key Words

Optimization, Pump-As-Turbines (PATs), Water Distribution Networks, Pressure Reducing Valves (PRVs)

1 Introduction

Over the last three decades, pressure management (PM) together with the rehabilitation of the infrastructure has proven to be one of the most efficient strategies for water losses reduction. In addition to the reduction of leakages, PM can also reduce the burst frequency of pipes (Vicente et al., 2016). Pressure reducing valves (PRVs) are usually installed at the entrance of district metered areas (DMAs) (Gomes et al., 2012). DMAs are the sectors of water distribution networks (WDNs) with defined boundaries where the flow that comes in and leaves is constantly metered for leakage monitoring. For smaller WDNs that are not divided into DMAs, PRVs are installed at the combination of pipes that maximize leakage reduction (Araujo et al., 2006).

Although the PM using conventional PRVs has many positive effects on the functioning of WDNs, the dissipated energy at the valves is irreversibly lost. In the last few years, a lot of researchers have been investigating technological and economic feasibility of replacing these valves with micro turbines or PATs (Fernández Garcia and Mc Nabola, 2020; Gallagher et al., 2015; Mc Nabola et al., 2014). The literature indicates large diurnal and seasonal flow and pressure variability, and the PM requirements, as the main technical challenges for replacing conventional valves with micro hydropower (MHP) plants (Fecarotta et al., 2018; Lydon et al., 2017).

There are studies which examined the use of conventional turbines (Coelho and Andrade-Campos, 2018; Corcoran et al., 2013) or specific hydropower devices (Sinagra et al., 2017) for this purpose, however the use of PATs prevails. Mainly this is due to the power output size of PRV sites within WDNs which is usually up to 100 kW (Delgado et al., 2019) and their significantly lower cost in this range comparing to the conventional turbines (Novara et al., 2019). Novara et al. (2019) suggested that the lower cost of PATs compared to the conventional turbines, influenced by their mass manufacturing, extends up to 300 kW.

The main barrier for wider implementation of PATs is the lack of knowledge about their behavior, as pump manufacturers still do not provide their performance curves (Novara and McNabola, 2018). As a result of this, many studies have been dealing with the predictability of PAT behavior. Experimental measurement of pumps in reverse mode has been shown to be the most accurate and reliable way to obtain the PAT curves, but these are expensive, time consuming and can require extensive specialist facilities (Barbarelli et al., 2017a). The application of computational fluid dynamics has been proven as a reliable alternative, but its application requires a 3D geometrical model of the machines (Bozorgi et al., 2013; Yang et al., 2012) . Thus, several semi-empirical equations have been proposed to correlate the Best Efficiency Point (BEP) of a unit in the pump and turbine mode (Alatorre-Frenk, 1994; Stepanoff, 1957; Yang et al., 2012) and to extrapolate the whole characteristic curves from machines BEPs (Novara and McNabola, 2018).

In the absence of flow regulation device and in order to attain similar PM to a PRV, three regulation schemes have been proposed in the literature for a MHP plant equipped with a PAT. The most common is hydraulic regulation (HR) where the PAT is installed in a hydraulic circuit consisting of two branches. The generation branch with a dissipating control valve (CV) in series to the PAT and the bypass branch equipped with another CV. The valve in series to the PAT dissipates the excess available pressure for smaller flows when the head drop introduced by the PAT is not enough to obtain the required downstream head while the bypass CV opens for larger flows to bypass part of it and to avoid larger head drops by the PAT than desired (Carravetta et al., 2012). An alternative regulation scheme employs electrical regulation (ER), where the generator's speed is changed using an electrical speed driver to match the load of an operating point, i.e., instantaneous flow and available head. This type of regulation lacks flexibility when the variations of flow and pressure are too large, as it may not be able to attain the set downstream head for all operating points. Moreover, it is inferior compared to HR in term of energy recovered (Carravetta et al., 2013). To improve the global efficiency of the plant the first two regulation schemes can be coupled (HER), representing the third scheme. In the study

performed by Fecarotta et al. (2018), the results showed only slight improvements in terms of the energy produced using the HER compared HR schemes. However, HER requires more complex control system and consequently larger investments.

1.1 Methodologies that consider the installation of PATs within Water Supply Networks

The methodologies that considered the installation of PATs within water supply networks (WSNs) can be classified into three groups. The methodologies from the first group consider a fixed operating point, i.e., constant flow and head through a PAT. The optimal PAT is usually the one whose resistance curve intersects the system curve closest to the desired operating point. These methodologies are suitable only for a limited number of locations in the transmission part of WSNs where the flow and pressure are constant or have very small fluctuations (Barbarelli et al., 2017b; Chapallaz et al., 1992).

Unlike the first group, the second group methodologies consider variable operation points at the PAT, meaning that a range of flows is passing through the PAT. In this case the head drop depends on the PAT's head loss curve and the type of regulation scheme implemented (Carravetta et al., 2013, 2012; Fecarotta et al., 2018; Lydon et al., 2017; Stefanizzi et al., 2018). These methodologies are usually applied to PRV sites. In common for all methodologies in this group is that these follow the traditional approach where the optimal PAT is hydraulically similar to a prototype machine whose performance curves are available and represents its scaled up or down version.

Finally, the methodologies from the third group are the ones that represent a part of larger optimization procedures that are applied to calibrated models of WDNs, focusing on selection of the optimal number and/or location of PATs within WDNs. The focus of these methodologies is more on the optimization algorithms rather than on the PAT selection and the behavior of PATs is usually simplified. Some methodologies simulated the presence of PATs as simple head drops and considered that the total flow always passes through PATs (Corcoran et al., 2016; Fecarotta and Mc Nabola, 2017), while others used approximated head loss curves but without any type of regulation (Lima et al., 2017; Tricarico et al., 2018). Additionally, the methodologies from this group (with exception of D-Town case study in Tricarico et al. (2018)) usually used only a single day hourly averaged flow and head patterns.

In terms of objective functions, the methodologies from the second group predominantly used the maximization of the energy recovered which is analogous to the maximization of the global efficiency of the plant. Carravetta et al. (2014) and Fecarotta et al. (2018) upgraded this objective function by adding terms that represent reliability and sustainability of the hydro plant. The economic variables such as Net Present Value (NPV) or Payback Period (PP) of the investment have not been used as the main objectives among the methodologies from this group. Carravetta et al. (2013) evaluated the costs and payback periods but the machines were selected by maximizing the plant's global efficiency. On the other hand the methodologies from the third group beside the maximization of energy recovery (Corcoran et al., 2016; Fernández Garcia and Mc Nabola, 2020; Lima et al., 2017) also used the maximization of NPV as the main objective (Fecarotta and Mc Nabola, 2017).

1.2 Aim of the paper

A large database of 38 PRV sites from Dublin and Seville WDNs with yearly recordings at time step of 15 min or less, was compiled for this study. The database was used to better understand the scale of hydropower sites within WDNs and to develop a novel comprehensive optimization-based PAT selection methodology. The novel optimization-based methodology employs the classical hydraulic regulation scheme with two control valves and a single-stage centrifugal PAT whose performance curves and maximal efficiency were predicted using the state of art models defined by Novara and Mc Nabola (2018) and Novara et al. (2017), respectively. To guide the model towards the optimal solution the Nelder-Mead simplex direct search optimization algorithm was used (Lagarias et al., 1998). Besides the optimization method used, the novelties of the proposed methodology are also reflected in the constraints imposed to the solution space which are defined only by the boundaries of the available single-stage centrifugal PATs on the market, and new formulation of the PAT's operation limits that

are based on its relative mechanical power. The accuracy of the model was validated using 23 experimental curves collected from the literature.

The proposed methodology was applied to real-world sites previously used in the literature to demonstrate the improvements introduced. Additionally, the study carried out two tests that have not previously been conducted in the literature. The first test examined the effects of using three independent single-objective functions on the optimal PAT, namely: maximization of energy recovery, maximization of NPV after 10 years and minimization of the payback period, respectively. Finally, the second test investigated the effects of using different operation limits on the optimal PAT. The goal of the conducted tests was to find out how much the theoretically optimal BEPs obtained using different objectives and different maximal operation limits differ from each other and if this can result in the selection of different commercially available pump families.

2 Methodology

2.1 Design variables

The performance characteristics of different centrifugal pumps or PATs can be defined with their BEPs, and the nominal impeller rotational speed (n). The aim of the proposed optimization model was to find the optimal values of the related three design variables for the considered sites. The rotational speed was considered a discrete variable with possible values of 1005, 1510, and 3020 rpm. The set of the rotational speeds was predetermined by the fact that the centrifugal pumps or PATs are usually coupled with asynchronous electric generators with either 3, 2 and 1 magnetic pole pairs. These generators are operating at constant speed to produce the electric current with synchronous frequency of 50 Hz. Also, the pump manufacturers usually provide the pump performance curve only for these speeds. In order to have the rotational speed different from these, additional equipment is needed such as a mechanical speed multiplier or an electrical speed driver (inverter) (Fecarotta et al., 2018) which complicate the installation and increase the cost. Like in the previous studies on this topic, the discharge and the head drop at the BEP were considered continuous (Carravetta et al., 2012; Lydon et al., 2017). This also means that the optimal solution is theoretical as there is a possibility that there is no commercial PAT with exactly the same values of BEP for considered n. However, the function of the theoretically optimal solution is to serve as a benchmark for identifying the most suitable commercial PATs in its proximity.

2.2 Constraints on the solution space

The methodologies available in the literature all followed the traditional approach where the most suitable machine for the selected site was obtained by scaling the prototype machine whose performance curves were available to the respective authors. In the optimization terminology this would mean that the constraints defined by the affinity equations are imposed on the solution space, i.e., that the BEP of the optimal scaled machines has to fall on the affinity curves. While this approach is adequative when the final machine is custom built like in the case of large turbines, in the case of MHP plants like the ones within WDNs, the final machine will be the one from a finite set of pumps/PATs' families available on the market for which the mass production cost can be availed. The PATs from this set are not all hydraulically similar meaning that these do not have the same value of turbine specific speed (N_s) based on either unit flow or unit power. Moreover, it is hard to anticipate the optimal value of the PAT's N_s for a PRV site where large flow and head variations are present and there is a regulation scheme. Even if this value is known, the characteristic curves of hydraulically similar machines probably are not available.

In the presented methodology the solution space of the PAT's BEP was constrained only with the boundaries that represent the available mass produced centrifugal PATs on the market for each rotational speed. The illustration of this concept is presented in Fig. 1. The boundaries for each available speed were defined by creating a database of centrifugal pumps from the catalogues of Etanorm and Etanorm-R models, that are classical end-suction centrifugal pumps (KSB, 2018). Their

BEPs as PAT were converted using the model defined by Yang et al. (2012) and affinity laws to adjust the speed to the turbine mode (e.g. from 1450 to 1510). The database included 58 different pump families and 150 different BEPs for three rotational speeds. Only the full impellers of these families were considered. The minimal values of BEP flow, head and specific speed amounted 1.49 l s^{-1}, 3.62 m and 3.74 rpm $(m^3\ s^{-1})^{0.5}(m)^{-0.75}$ while the maximal values were 513.1 l s-1, 398.06 m and 102.89 rpm $(m^3\ s^{-1})^{0.5}\ (m)^{-0.75}$ respectively.

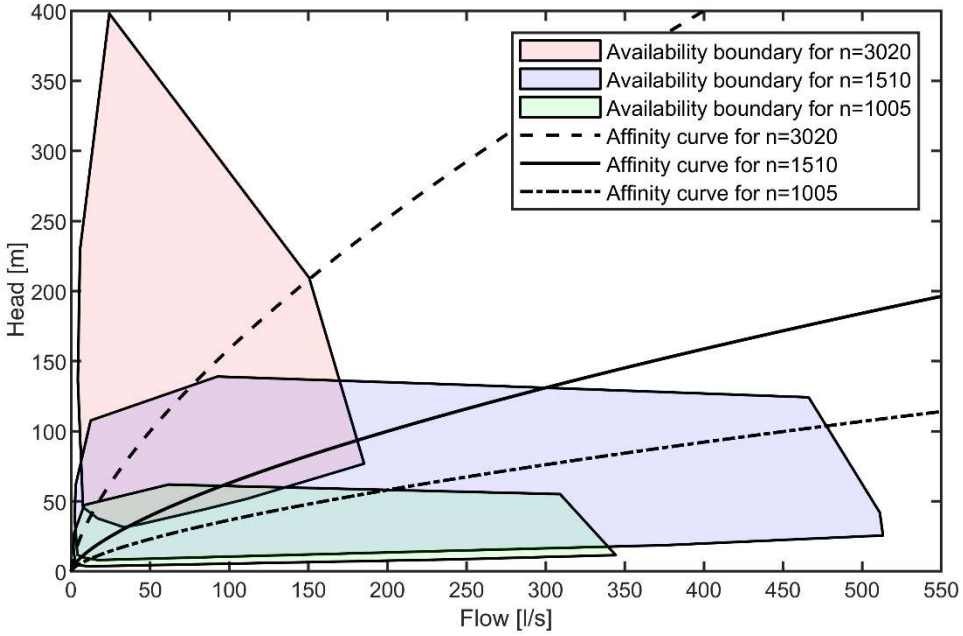

Fig. 1. Boundaries of available PATs as constraints to solution space.

2.3 Energy recovery objective function

The energy recovery objective function has the following form:

$$\underset{Q_{BEP},H_{BEP}}{maximize}\, E\,(n) = \sum_{i=1}^{N} \rho g Q_i^{PAT} H_i^{PAT} \eta_i^{PAT} \Delta t \quad (1),$$

where $E\,(n)$ [MWh $year^{-1}$] is the energy produced for the selected rotational speed n [rpm], N – number of operating points; ρ [kg m^{-3}] - water density; g [m s^{-2}] – gravitational acceleration; Q_i^{PAT} [m^3 s^{-1}] – flow through the PAT; H_i^{PAT} [m] – head drop at the PAT; η_i^{PAT} [-] – part load efficiency of the PAT for Q_i^{PAT} and Δt [h] – time step duration.

The algorithm for evaluating the energy recovery function consists of the following steps:

1. In the initial step the algorithm checks if the solution is inside of the boundaries of the available PATs for the selected speed (see Fig. 1.). If the solution is outside the boundaries for that speed the algorithm sets energy generation to zero, E=0. This step is an alternative to classical penalty functions as the optimization algorithm used (see subsection "Optimization algorithm") does not incorporate constraints. The penalty function was implemented this way because for very small flows it can happen that the optimization algorithm converges to negative flow values where it is not possible to evaluate the objective function. A drawback of this formulation is that the starting point has to be inside of the boundaries for the considered n.

2. The algorithm calculates specific speed based on the unit flow:

$$N_s = n\frac{Q_{BEP}^{0.5}}{H_{BEP}^{0.75}} \quad (2),$$

which unifies all design variables and represents a key performance parameter of a PAT.

3. The algorithm defines polynomials for the extrapolation of the head loss and power curves based on the design variables and model defined by Novara and McNabola (2018).

$$\frac{H_i^{PAT}}{H_{BEP}} = a\left(\frac{Q_i^{PAT}}{Q_{BEP}}\right)^2 + b\left(\frac{Q_i^{PAT}}{Q_{BEP}}\right) + c \quad (3),$$

with the values of coefficients $a = 1.160$, $b = 0.0099N_S + 1.2573 - 2a$ and $c = 1 - a - b$, and

$$\frac{P_i^{PAT}}{P_{BEP}} = d\left(\frac{Q_i^{PAT}}{Q_{BEP}}\right)^2 + e\left(\frac{Q_i^{PAT}}{Q_{BEP}}\right) + f \quad (4),$$

with values of coefficients $d = 1.248$, $e = 0.0108N_S + 2.2243 - 2d$ and $f = 1 - d - e$. The power at BEP was assessed as $P_{BEP} = \rho g Q_{BEP} H_{BEP} \eta_{max}$, by predicting η_{max} using an equation defined by Novara et al. (2017) based on experimental data of 280 radial PATs:

$$\eta_{max} = 0.89 - \frac{0.024}{Q_{BEP}^{0.41}} - 0.076\left(0.22 + ln\frac{N_s}{52.933}\right)^2 \quad (5).$$

Novara and McNabola (2018) improved the accuracy of their extrapolation model comparing to similar models of this kind (Barbarelli et al., 2017a; Derakhshan and Nourbakhsh, 2008; Fecarotta et al., 2016; Pugliese et al., 2016), by introducing variable polynomial coefficients that depend on the value of *Ns*. They proved and quantified the hypothesis proposed by Chapallaz (1992) that the slope of the relative characteristics curves increases with the increase in the value of N_s.

4. This step introduces the operation limits, i.e., the minimal and maximal flow that is allowed to pass through a PAT. These limits are rarely mentioned in the literature. The proposed methodology here sets the limits to relate the relative mechanical power produced by the PAT, namely, $P_{rel}(Q_{min}^{PAT}) = 0.375$ for the lower and $P_{rel}(Q_{max}^{PAT}) = 1.5$ for the upper limit. Clarification about these limits is presented in the following subsection.

5. This step implements the HR strategy and assesses how much energy is being effectively produced by the PAT in each time step, i.e., for each operating point (Q_i, H_i). The aims of the regulation strategy are the following: 1) maximize energy produced; 2) attain the same downstream head as the PRV predecessor; 3) prevent the generator from starting to work as a motor; 4) prevent excessive torques and potential overheating of the generator; these apply to each time step. To attain the same downstream head as the PRV predecessor the algorithm considers only the exploitation of the excess head – H_i, available at the PRV. This head is obtained by subtracting the recorded upstream and downstream heads at the PRV. To achieve these aims the algorithm first extrapolates the complete head loss curve from the considered BEP alternative within the limits defined in step 4, using the extrapolation model defined at step 3. Based on the position of each operating point in the Q-H space (marked with crosses in Fig. 2) in respect of the created head loss curve, all of the operating points can be grouped into four regulation regions. This is done based on how much flow will be directed through the PAT and which CVs need to be active to achieve such regulation. These four regions are illustrated in Fig. 2 using four different colors. Mathematically, these four regions can be characterized using the following equations:

$$Q_i < Q_{\min}^{PAT} \; or \; H_i < H_{min}^{PAT} \rightarrow E_i = 0 \quad (6),$$

$$Q_{min}^{PAT} \leq Q_i < Q_{max}^{PAT} \; and \; H_i \geq H^{PAT}(Q_i) \rightarrow E_i = \rho g Q_i H^{PAT}(Q_i) \eta_i^{PAT}(Q_i) \Delta t \quad (7),$$

$$H_{min}^{PAT} \leq H_i < H_{max}^{PAT} \; and \; Q_i > Q^{PAT}(H_i) \rightarrow E_i = \rho g Q^{PAT}(H_i) H_i \eta^{PAT}(Q^{PAT}(H_i)) \Delta t \quad (8),$$

$$Q_i \geq Q_{max}^{PAT} \; and \; H_i \geq H_{max}^{PAT} \rightarrow E_i = \rho g Q_{max}^{PAT} H_{max}^{PAT} \eta^{PAT}(Q_{max}^{PAT}) \Delta t \quad (9).$$

For the operating points that satisfy one of the inequalities defined in Eq. 6 (green crosses in Fig. 2), the entire flow needs to be bypassed and consequently there is no electricity generation. If the flow is too low ($Q_i < Q_{\min}^{PAT}$), it needs to be bypassed to prevent the potential operation of the

generator as a motor as the shaft mechanical power is not sufficient even to create the nominal electromagnetic flux. For the operating points with the larger flows but with excess head lower than H_{min}^{PAT}, the necessary bypassing to avoid the excessive head drops at the PAT would lead to the same phenomena. For the operating points that satisfy both inequalities defined in Eq. 7 (blue crosses in Fig. 2), the entire flow is directed through the generation line in the PAT, creating head loss at the PAT according to its head loss curve $(H^{PAT}(Q_i))$, while the excess head is dissipated by the CV in series $(H_i - H^{PAT}(Q_i))$. For all the operating points that satisfy both inequalities defined in Eq. 8 (red crosses in Fig. 2), a part of flow needs to be bypassed to avoid head drops larger than the excess head. The exact flow that should be directed through the PAT to maximize the energy recovery and avoid excessive head drops is the flow from the PAT head loss curve that corresponds to the available excess head $(Q^{PAT}(H_i))$. Finally, when both flow and available head are higher than the maximum permissible values (black crosses), both CVs are active allowing the flows higher than Q_{max}^{PAT} to be bypassed. The CV in series dissipates the head larger than H_{max}^{PAT}. This is to prevent potentially dangerous torques and overheating of the generator.

6. Final step represents the summation of energy generated in each time step using Eq. 1 and the PAT's flows and heads determined in the previous step, thus calculating the yearly energy generated.

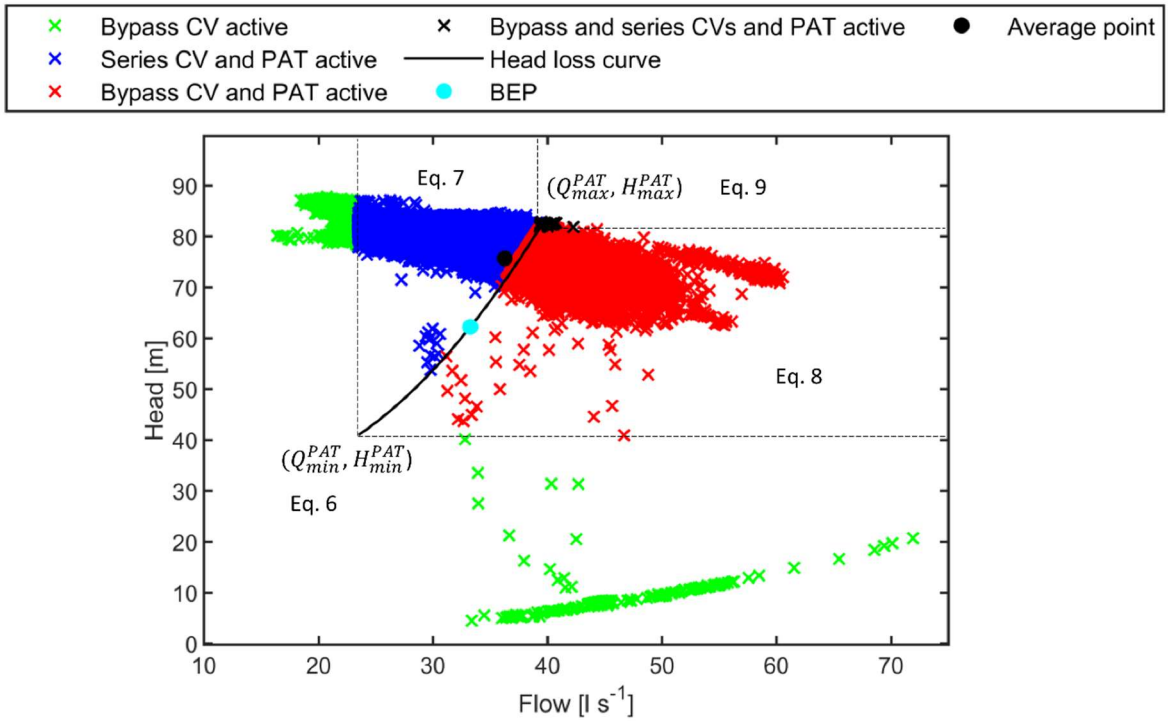

Fig. 2. Yearly Q-H operating points at Site 13 within Dublin WDN, colored based on regulation regions.

As the methodology uses the semi-empirical models presented in step 3 to predict the PAT behavior, its accuracy is proven only for the range of PATs based on which the models were defined. Both of the models include PATs with N_s between 5-150 rpm (m^3 s^{-1})$^{0.5}$ (m)$^{-0.75}$, but only a few with N_s larger than 100. The largest BEP flow in the set used to define maximal efficiency equation was 500 l s^{-1}, while in the set for the extrapolation model it was 320 l s^{-1}. The availability boundaries presented in Fig. 1 are in line with these limitations, except for n=1510 where the maximal allowed flow is larger than the maximal flow used to define the extrapolation model. However, the authors assume that the accuracy of this model is acceptable for the flows up to 500 l s^{-1}.

Also, the function for predicting maximal efficiency defined with Eq. 5 is smooth meaning that it considers only the PATs with full impellers. In addition, this equation includes only the mechanical efficiency.

2.4 PAT's operation limits based on its relative mechanical power

A possible reason why the majority of the studies have not mentioned the limits was that these used very short time series data, where the flow and head variations were less prominent and consequently for the selected machine these limits were never reached. Consequently, all operating points would fall in the regions defined with blue and red crosses in Fig. 2. However, the yearly time series of flow and head at three examined sites in this study suggested that their variations in normal operations are such that these limits have to be introduced.

Fontana et al. (2016) set the maximal flow through the PAT to relate the efficiency of 0.4, arguing this as a mean to avoid the cavitation. Other authors suggested a minimum value of total required exhausted head to avoid this phenomena (Carravetta et al., 2018; Chapallaz et al., 1992). Based on the research carried out by Chapallaz et al. (1992), and the fact that the back pressure required to be maintained downstream of PRVs within WDNs, which is rarely below 15m, cavitation can be an issue only for very small PATs with very curved impeller vanes which tend to cavitate earlier.

Although, Chapallaz (1992) considers only fixed operation of a PAT, the author also introduces the theoretically possible range of operation of a PAT. The upper limit of this range was determined with maximal permissible torque, i.e., maximal shaft resistance curve. The maximal torque is proportional to maximal shaft power. The author suggested that the PATs should be able to sustain torques two times larger than torques at BEP, but also that PATs at the lower end of the series are often overdesigned as the standard shaft design is being used for a compete series of pumps. As it was mentioned previously, in this paper the maximal flow was limited to relate relative mechanical power of $P_{rel}(Q_{max}^{PAT}) = 1.5$

A few authors suggested that any flow larger then BEP should be bypassed (Fernández Garcia and Mc Nabola, 2020). Limiting the maximal flow to BEP would not maximize the energy recovery as the power curves are strictly increasing curves at least up to 1.4*Q_{BEP} (Novara and McNabola, 2018), and sometimes even up to 2*Q_{BEP} (Fontana et al., 2016).

The bottom line for the minimal flow is to prevent that the generator starts working as a motor for very small flows. Although the induction generators operate with high efficiency over a wide range of the part loads, the studies of the part load efficiency suggest that it can drop significantly at values of 20% of its nominal load (Deprez et al., 2006). In the aforementioned study by Fontana et al. (2016) the mechanical power attained for the maximal flow was more than 5 times larger than the power attained for BEP flow. In this paper the lower limit for flow was set to correspond to 20% of generator's nominal load. If the maximal load to the generator ($P_{rel}(Q_{max}^{PAT}) = 1.5$) represents 80% of its nominal capacity as a motor, as suggested by Williams (1996) in order to avoid overheating and reliability issues, then using proportion 20% of the load corresponds to relative power of $P_{rel}(Q_{max}^{PAT}) = 0.375$. This formulation results in narrower relative permissible operating range for the PATs with higher values of N_s, as the consequence of the steeper relative power curves (see Fig. S1).

The lower and upper limits of flow passing through a PAT defined in this paper should be considered as the general limits for the whole application range while the final limits should be tuned once all parts of the plant are selected.

2.5 NPV and Payback Period Objective Functions

Besides the maximization of the energy produced, two economic variables were used to pursue the optimal values of the design variables, namely NPV after 10 years and payback period (PP) of the investment. The economic variables have not previously been used by methodologies for selecting

theoretically optimal PAT, i.e., its BEP and n. For each rotational speed, the following formulas have been used to evaluate the economic objectives:

$$NPV_{10}(n) = -TIC + \sum_j^Y \frac{E \cdot e_{up} - OMC}{(1+r)^j} \quad (10)$$

$$PP(n) = \frac{TIC + OMC}{E \cdot e_{up}} \quad (11)$$

where TIC [€] are the total installation costs; E [MWh year^{-1}] is the energy produced per year; e_{up} [€ MWh^{-1}] is the electricity unit price when sold to the grid [90€ per MWh was assumed in this work (Electric Ireland, n.d.)]; OMC [€] are the annual operation and maintenance costs ;j is the year since investment; Y=10 is the number of years for which *NPV* is calculated; and r [-] is the discount rate [assumed value of 0.05 (Fecarotta and Mc Nabola, 2017)]. The total installation costs TIC, were calculated as a summation of $C_{PAT+gen}$ [€], the PAT and generator assembly cost, and OIC [€] other installation costs:

$$TIC = C_{PAT+gen} + OIC \quad (12)$$

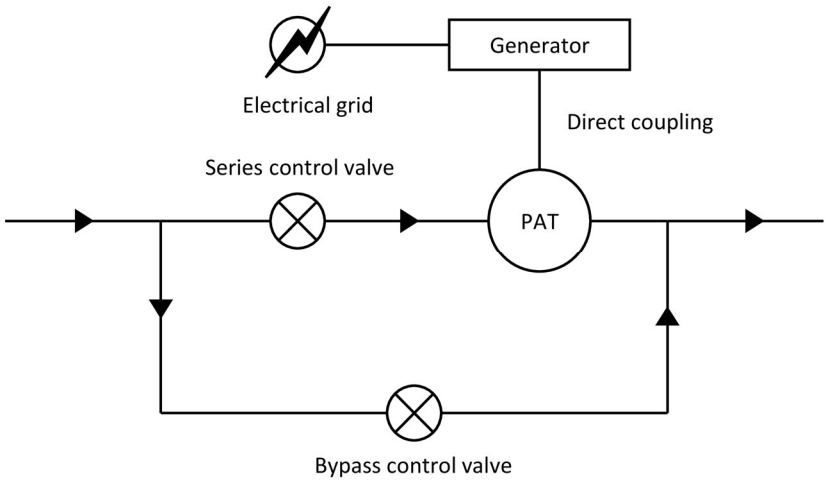

Fig. 3. Hydraulic regulation installation scheme.

A model developed by Novara et al. (2019) was used to predict the cost of a PAT coupled with induction generator. This model takes into account that the same pump unit operating in the turbine mode requires a generator of larger nominal power, and that the generators with higher number of the magnetic pole pairs (pp) are more expensive:

$$pp = 1\ (n = 3020):\ C_{PAT+g} = 11{,}913.91 \cdot Q_{BEP}\sqrt{H_{BEP}} + 1{,}289.92 \quad (13)$$

$$pp = 2\ (n = 1510):\ C_{PAT+gen} = 12{,}717.29 \cdot Q_{BEP}\sqrt{H_{BEP}} + 1{,}038.44 \quad (14)$$

$$pp = 3\ (n = 1005):\ C_{PAT+gen} = 15{,}797.72 \cdot Q_{BEP}\sqrt{H_{BEP}} + 1{,}147.92 \quad (15),$$

where Q_{BEP} [m^3 s^{-1}] and H_{BEP} [m] are the flow and head drop of the PAT at its BEP. OIC were associated with HR control system (including two control valves see Fig. 3), commissioning, civil works, grid connection, additional hydraulic equipment and other project costs. The value of OIC, was assessed implicitly from $C_{PAT+gen}$:

$$OIC = (1 - 0.26)\frac{C_{PAT+gen}}{0.26} \quad (16).$$

Equation 16 suggests that OIC correspond to 74% of TIC. This assumption is based on the study conducted by Fernández García et al. (2019) which analyzed nine different real world PAT installations in WDNs, finding that the cost of PAT plus generator assembly represented 26% of TIC on average.

Across the literature the magnitude of OMC was shown to vary significantly. Their magnitude varied from being neglected (Fecarotta et al., 2014; Fecarotta and Mc Nabola, 2017) to being 15% of the total installation costs, annually (Fernández Garcia and Mc Nabola, 2020; Tricarico et al., 2018). In between were the studies by Novara and McNabola (2018); Coelho and Andrade-Campos (2018) and Colombo and Kleiner (2011); where these costs were defined as 5% of C_{PAT+g} , 10% of the project's total annual income and 2000$, respectively. In this paper these costs were assessed as the median value of 15% of C_{PAT+g} .

When a solution point (Q_{BEP}, H_{BEP}) is outside the availability boundaries for the speed n, the algorithm sets NPV_{10} to -10^6 €, and PP to 100 years.

2.6 Optimization algorithm

For the energy recovery objective function the optimization problem described above can be formulated as follows:

$$\begin{aligned} \underset{Q_{BEP},H_{BEP}}{maximize}: \quad & E(n) = \sum_{i=1}^{N} \rho g Q_i^{PAT} H_i^{PAT} \eta_i^{PAT} \Delta t \\ s.t. \quad & n \in \{1005, 1510, 3020\} \\ & (Q_{BEP}, H_{BEP}) \in Boundary(n) \end{aligned} \quad (17).$$

The problem formulation for the other two objectives is the same as in Eq. 17 except in the case of the PP objective for which the goal is to minimize PP. For a single rotational speed n, the problem formulated in Eq. 17 is nonlinear subject to linear constraints defined using availability boundaries. Because of the piecewise nature of the energy recovery function defined in Eq. 6-9 and due to the discrete nature of the PRV operating points, the objective functions are discontinuous and hence non-differentiable. As it will be seen in the result section, the described problem is a local problem.

Considering the problem characteristics, the Nelder-Mead Simplex Direct Search (NMSDS) algorithm has been chosen to solve the optimization problem (Lagarias et al., 1998). The NMSDS algorithm is derivative-free heuristic search method suitable for nonlinear non-smooth problems. It belongs to the class of direct search methods whose convergence is based on function comparison. As the algorithm does not incorporate constraints, the boundary constraints are implemented through the penalty function defined in step 1 of the energy recovery function.

The method uses the concept of a three-point simplex for a 2D-problem. The flowchart of the algorithm is presented in Fig. 4. The starting point (Q_{start}, H_{start}) can be anywhere within the availability boundary for the selected rotational speed. The average operating point is a good initial guess if it is within the boundary. As can be seen in the chart, the algorithm tries to replace the worst element of the simplex ($\boldsymbol{x}_{k+1}$), with a better solution by reflecting and contracting through the centroid ($\boldsymbol{x}_m$) of the remaining simplex points. If none of the alternatives is better that the worst point of the simplex, the algorithm shrinks the simplex towards the best point. The advantage of the NMSDS algorithm is that it requires less function evaluation in each iteration then some other heuristic methods. However, it is not suitable for global optimization problems.

All the simulations were carried out in the MATLAB programming environment.

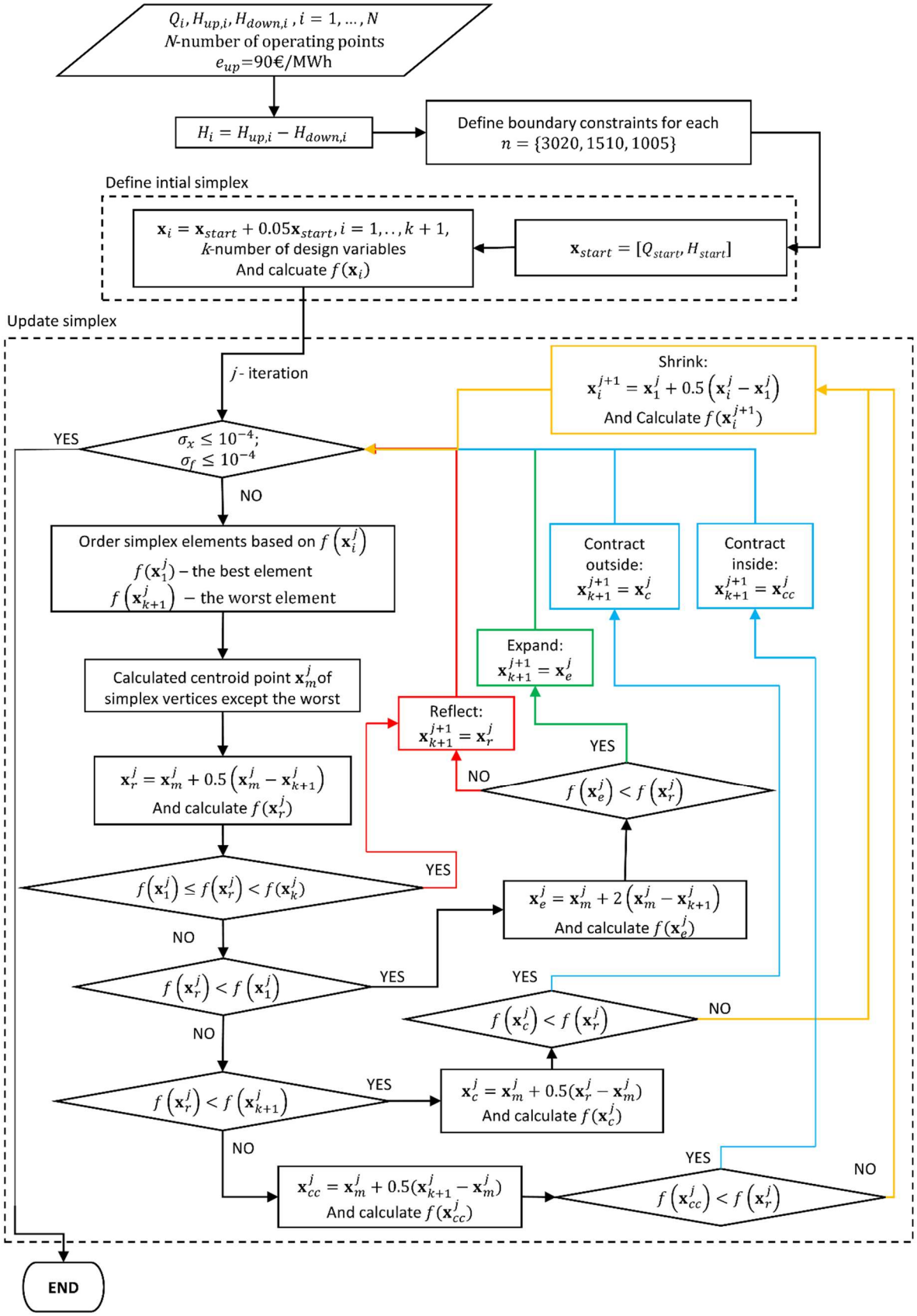

Fig. 4: Optimization algorithm flowchart

3 Validation

As the pump manufacturers do not provide the information about pumps behavior in turbine mode, researchers and practitioners have to rely on some of the prediction models developed in the literature. All PAT performance prediction models induce certain errors. To quantify the errors of their models the developers usually use the accuracy metrics such as root mean square error (RMSE) and coefficient of determination (R^2) (Barbarelli et al., 2017a; Derakhshan and Nourbakhsh, 2008; Fecarotta et al., 2016; Novara and McNabola, 2018; Pugliese et al., 2016). These metrics do not provide an explicit answer about the magnitude of error in the assessment of energy produced. Furthermore, the methodologies that are focused on selecting a PAT to replace a PRV which would operate with variable flow and head conditions, usually couple several of these models where each embeds its error. Previous methodologies in this field omitted to quantify this cumulative error.

As it was explained in the previous section the proposed methodology employs two models: a model for extrapolation of complete head loss and power curves from the machine's BEP (Novara and McNabola, 2018) and a model for prediction of the machine's maximal efficiency at the BEP (Novara et al., 2017). Also, a model developed by Yang et al. (2012) has been used to define the boundaries of the available models for each rotational speed. To quantify the cumulative error in the assessment of energy recovery of the proposed methodology 23 experimental PAT curves of centrifugal PATs have been gathered from the literature (Alatorre-Frenk, 1994; Barbarelli et al., 2017a; Calado, 2014; Sebastião, 2017).

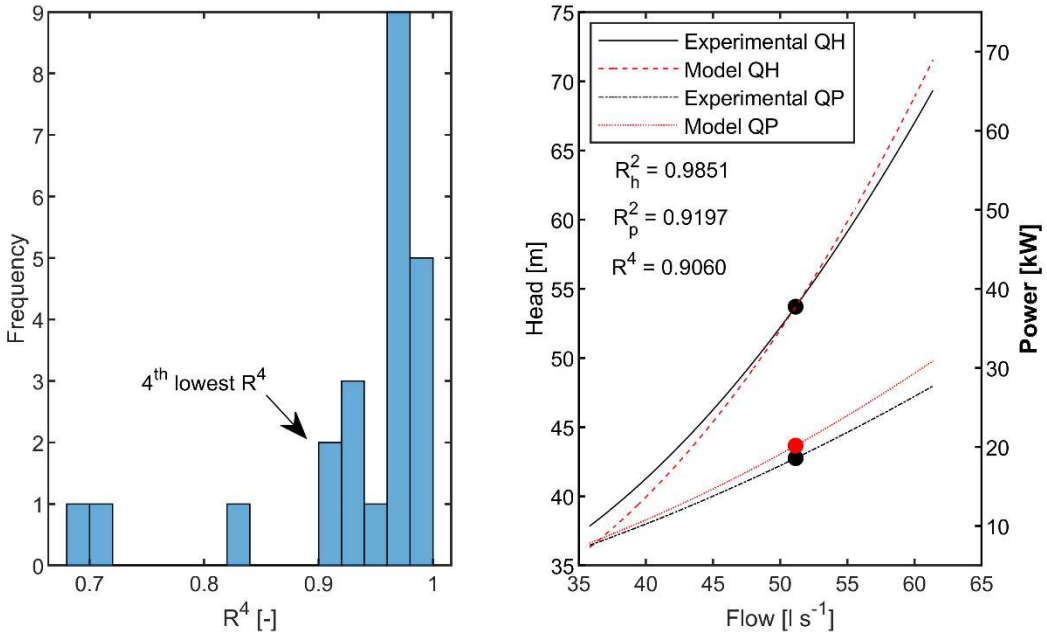

Fig. 5. a) Distribution of R^4 for 23 PAT curves from the literature; b) Experimental and modelled head loss and power curves for the PAT with the 4th lowest value of R^4

Two tests were carried out. In the first test, the BEP flow and head of the modelled curves were considered ideal, i.e., the same as the experimentally obtained ones. This way only the accuracy of the extrapolation and the model for predicting the maximal efficency in the assessment of energy recovery was quantified. Firstly, the R^2_h (R^2 for head loss curves) and R^2_p (R^2 for power curves) were calculated for all 23 PATs. Some PATs had better fit for the head loss curves but worse for the power curves, i.e., the PAT that had the worst accuracy by R^2_h was not the worst by R^2_p. As both of these types of curves influence the accuracy of energy reovery assessment, a joint metric that couples their accuracies was necessary to sort the 23 PATs. Consequently, the metrics R^2_h and R^2_p were multiplied

creating $R^4 = R^2_h R^2_p$. Distribution of this metric is displayed in Fig. 5a, and shows three PATs that had significantly lower values of R^4 than the other 20 PATs. Considering these three PATs as outliers, the PAT with the 4th lowest value of R^4, amounting to 0.906 was chosen to quantify the cumulative error in the assessment of energy recovery induced by the models (see Fig. 5b). Using the selected PAT, the energy recovery was assessed for three out of 38 sites from the aforementioned PRV database whose operating points were in the proximity to the PAT's head loss curve. A detailed description of the PRV database is presented in the following section. The relative errors in the assessment of energy recovery were 3.62, 5.74 and 7.5%. These values prove the high accuracy in finding the theoretically optimal BEP. The error could be larger for the sites whose operating points are far away from the PAT's head loss curve as all of the operating conditions would take place in the part-load or over-load part of the curves where discreptancy between the model and the experimental curves is the largest.

In the second test the accuracy of the Yang et al's model (2012) in the prediction of the PAT BEPs from the pump BEPs was assessed. Previous studies pointed out this model as one of the best in the literature (Novara, 2020). Fig. 6 presents the relative discrepancy between the predicted BEPs(empty circles) and the experimetally obtained BEPs(solid circle) for 23 PATs. It can be seen from the figure that the absolute relative error in predicting BEP flow, ranged from 0.04% to 19.78% with an average of 6.42%. On the other hand, the relative absolute error in predicting BEP head, ranged from 0.26% to 28.69% with an average of 10.28%. The errors of this magnitude in predicting the PAT BEP could induce significant errors in the assessment of energy recovery.

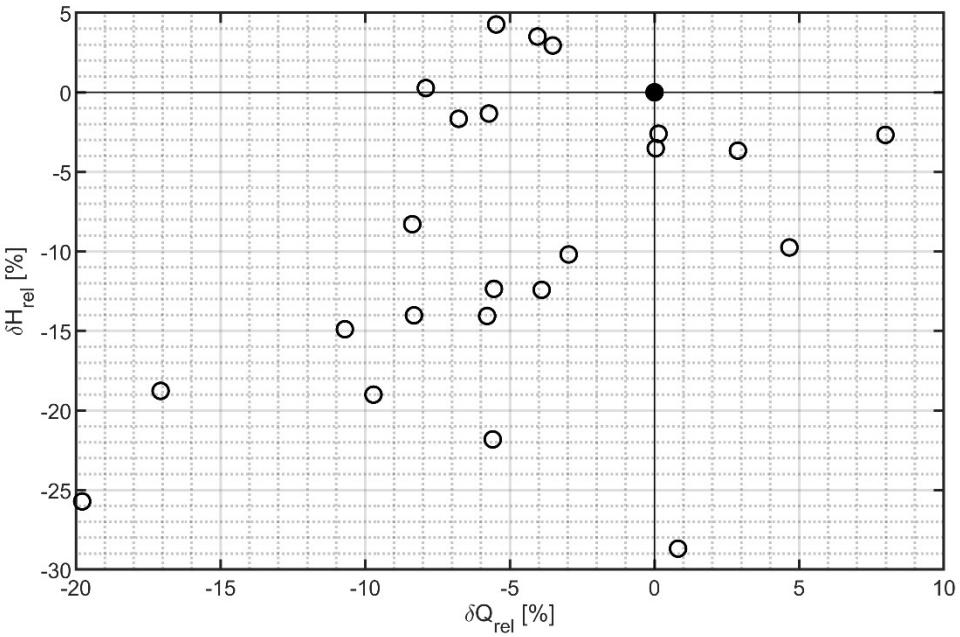

Fig. 6. Distribution of relative errors in prediction of BEP flow and head using Yang et al.'s model (2012).

4 Results and discussion

4.1 PRV database

A database of 38 real world PRV sites with yearly recordings of flow and head upstream and downstream the valves were available for this study. The set of valves included 30 PRVs from Dublin City WDN (Ireland) and 8 PRVs from Seville WDN (Spain). Flow and heads at Dublin valves were recorded at 15 min intervals for a duration of 420 days in the period between Jun 2010 - Aug 2011, while the ones in Seville were recorded at 5 min intervals and duration of 365 days for the period between Dec 2017 – Dec 2018. In the both subsets, majority of the valves had fixed downstream head

profiles but there are some with different head profiles for day and night, and also with flow-based head profiles as well.

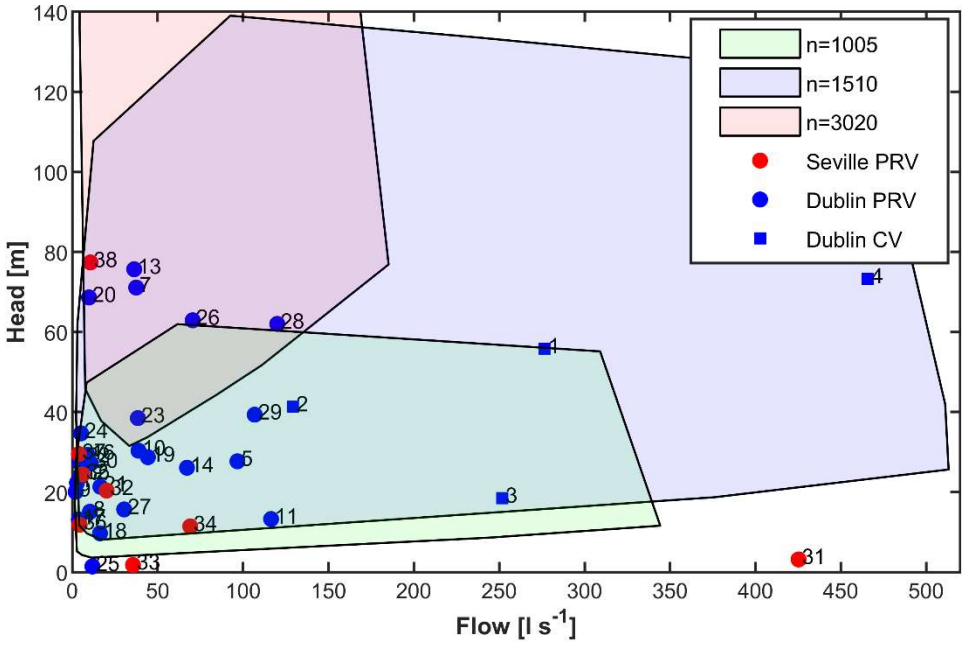

Fig. 7. Average operating points of 38 PRV sites with availability boundaries.

The available database was used to better understand the scale of hydropower sites within WDNs and to find suitable technology that can exploit their potential. Fig. 7 presents average operating points of all PRVs from the database (average flow and excess head), together with availability boundaries of the centrifugal PATs. None of the valves had excess head greater than 80 m and majority of sites had flow smaller than 120 l s^{-1}. The size of the sites in this database are in agreement with the sizes previously reported in the literature (Delgado et al., 2019). Fig. 7 confirms the suitability of radial and mixed flow centrifugal PATs for application at vast majority of PRV sites within WDNs. Three PRV sites that were outside of the boundaries have very small available head and their excess energy would be hard to exploit with any turbine technology.

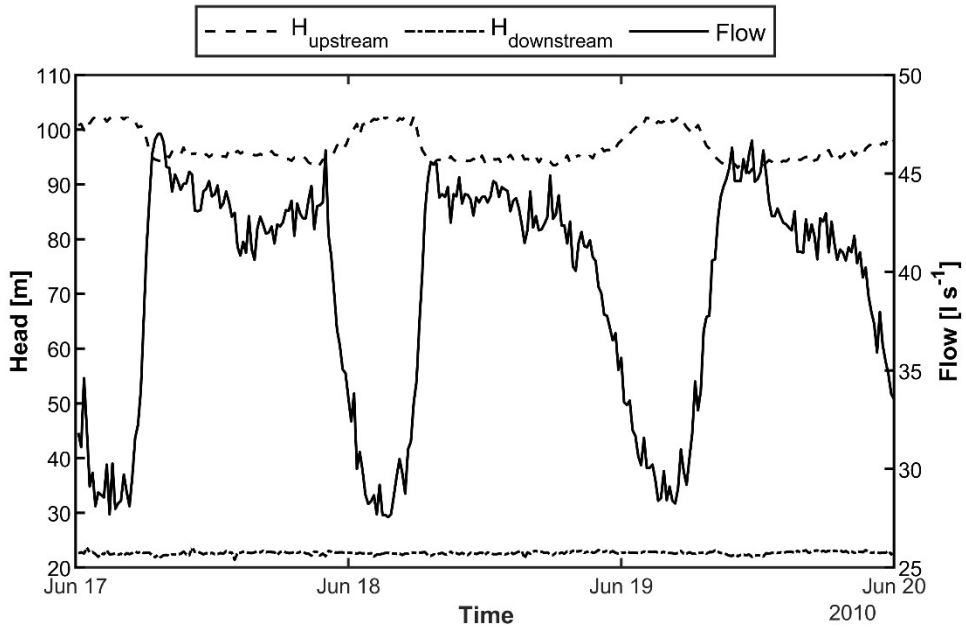

Fig. 8. Flow and head recordings at Site 13 for the first three days of the sample.

4.2 Effects of different objectives on the optimal BEP

From the previously mentioned PRV database three sites have been selected to examine the effects of selecting different objectives on the theoretically optimal PAT and final selection of the commercial pump family. The recordings of upstream and downstream head and flow at one of these sites (Site 13) for the first three days of the sample is presented in Fig. 8.

Fig. 9 presents the contour plots of the three examined objectives for each examined speed, for Site 13. The contour plots indicate that the examined optimization problem defined with equations 17 and analogues problems with NPV_{10} and PP objectives are indeed local problems, thus proving the suitability for usage of Nelder-Mead algorithm. The numerical values of theoretically optimal solutions for all three sits are presented in Tab. 1. The theoretical solutions can be regarded as upper bounds in the cases of energy recovery and NPV_{10} objectives and lower bound in the case of PP objective.

Tab. 1. Effects of different objective functions on the optimal BEPs for three PRV case studies

	Site 13			Site 28			Site 1		
Objective	*max(E)*	*max(NPV_{10})*	*mini(PP)*	*max(E)*	*max(NPV_{10})*	*mini(PP)*	*max(E)*	*max(NPV_{10})*	*mini(PP)*
Q_{BEP} [l s^{-1}]	33.25	32.10	26.08	111.98	105.05	77.77	250.63	232.78	151.08
H_{BEP} [m]	62.21	59.20	56.82	55.34	50.06	46.20	46.39	42.41	41.64
n [rpm]	3020	3020	3020	3020	3020	3020	1510	1510	1510
Ns [rpm (m^3 s^{-1})$^{0.5}$ m$^{-0.75}$]	24.86	25.35	23.56	49.81	52.01	47.53	42.53	43.84	35.80
η_{max} [-]	0.77	0.77	0.76	0.83	0.83	0.82	0.85	0.85	0.84
P_{BEP} [kW]	15.65	14.38	11.00	50.41	42.64	28.93	96.68	81.96	51.57
η_{global} [-]	0.62	0.61	0.55	0.66	0.65	0.55	0.66	0.66	0.51
E [MWh year^{-1}]	143.81	143.31	129.28	416.51	412.87	350.26	874.15	866.93	664.74
NPV_{10} [€ year^{-1}]	77854	78413	71672	233338	236156	205444	493662	500800	394722
PP [years]	1.36	1.31	1.25	1.20	1.09	0.96	1.16	1.04	0.90
Q_{BEP}/Q_{ave} [-]	0.92	0.89	0.72	0.93	0.88	0.65	0.91	0.84	0.55
H_{BEP}/H_{ave} [-]	0.82	0.78	0.75	0.89	0.81	0.74	0.83	0.76	0.75
Optimal commercial family	50-160, n=3020, D=174	50-160, n=3020, D=174	50-160, n=3020, D=174	100-160, n=3020, D=185	100-160, n=3020, D=185	80-160, n=3020, D=174	200-330, n=1510, D=330	200-330, n=1510, D=330	150-315, n=1510, D=334

Surprisingly, not many studies on this topic relate their optimal solution to the average operation point, i.e., average flow and excess head at the examined sites. In the study carried out by (Stefanizzi et al., 2018), the authors suggested that the BEP of a PAT (in the alternative with 1 PAT) should be as close as possible to the average point to maximize energy recovery. The authors supported this hypothesis with the fact that this point has the highest frequency of occurrence. On the other hand, the results of the study by Lydon et al. (2017) suggested that the design flow which will maximize energy recovery should be between 10% and 30% smaller than the average flow depending on the site (in the alternative with 1 PAT). They explained that the design flow should be small enough to have a high frequency of larger flows occurrence but big enough to capture most of the available energy. In this paper the theoretically optimal BEPs that will maximize the objectives are the result of the optimization procedure. The results presented in Tab. 1 indicate that the average BEP flow and available head, across the three considered valves, that would maximize the energy recovery, NPV and PP objectives, amounted 92% and 85%, 87% and 78% and 64% and 75% of the valves' average operating points, respectively. It can be also noticed that these ratios do not change much across the valves except in the case of Q_{BEP}/Q_{ave} ratio for the minimization of PP, which seems to decrease with the increase of the average operation flow at the valves.

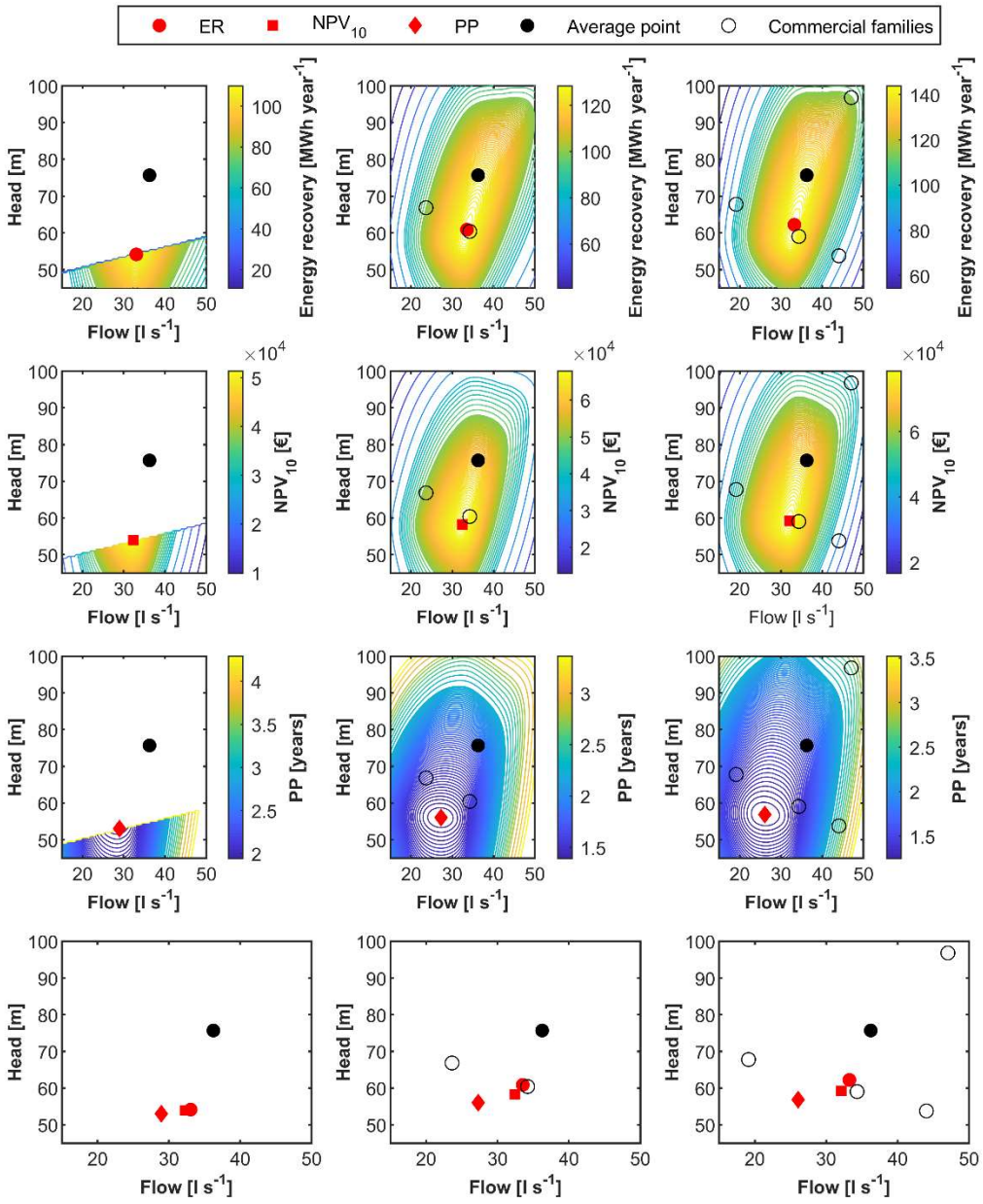

Fig. 9. Contour plots of Site 13: a) max(E) n=1005; b) max(E) n=1510; c) max(E) n=3020; d) max(NPV) n=1005; e) max(NPV) n=1510; f) max(NPV) n=3020; g) min(PP) n=1005; h) min(PP) n=1510; i) min(PP) n=3020; j) - l) Optimal BEPs of the objectives with available commercial families for each rotational speed.

As the PAT selection charts do not exist, to find the best commercial pump family alternative for the considered site, the theoretically optimal BEP in turbine mode should be converted into related BEP in pump mode using Yang et al.'s (2012) model or any similar conversion models. Using the obtained BEP in pump mode from the pump selection charts the near optimal commercial pump families can be selected. The BEPs of the pumps in proximity to the theoretically optimal BEP should be converted in turbine mode to assess the exact values of the objectives. The BEPs of the commercial Etanorm pumps that were in proximity to the optimal BEP for three considered sites are presented in Tab. S1-S3. For Site 13, these BEPs are also presented as empty circles on contour plots in Fig. 9.

Tab. 1 indicates that in case of Site 13 the best commercial family was the same regardless of the objective. On the other hand, in the cases of Sites 28 and 1 the best solutions obtained based on energy recovery and NPV_{10} objectives differed from the solution obtained using PP objective. Although, the best commercial alternatives in the cases of all examined sites and objectives, all were of the optimal speed, from Tab. S1-S3 it can be seen that the second best solution was of a different speed, which suggests that because of discrete nature of the commercial families all speeds should be always examined.

However, it should be noted that since recently some pump manufactures started selling their units to be used in turbine mode, even that the performance in turbine regime is still not available (e.g. KSB). In other words, the theoretically optimal BEP can be provided to the manufactures to suggest the best commercial alternative. This way, the potentially wrong commercial solutions resulting from significant errors of the conversion models such Yang's can be avoided.

4.3 Effects of different PAT's operation limits on the optimal BEP and energy recovery

In the literature, different studies used different values for the maximal operating flow of a PAT. Fernández Garciá and Mc Nabola (2020) and Lydon et al. (2017) implemented HR in their methodologies that bypasses every flow larger than BEP flow. In the experimental study by (Fontana et al., 2016) that investigates real time control strategy of a prototype that maximizes energy produced, the authors set the maximal flow through the PAT (referred as desired flow in the study) to a value two times larger than BEP flow. Carravetta et al. (2014) and Fecarotta et al. (2018) introduced the minimal and maximal flow through the PAT implicitly using a reliability parameter in their objective function. This parameter takes into account that a pump/PAT is more prone to failure if it works away from BEP. This parameter was defined with a bell curve that has the maximum of one at BEP flow and zeros at no flow on the left side and flow two times bigger than BEP flow at the right side. However, the studies did not indicate if the reliability curve defined as this was created on a premise that a PAT works for the whole duration away from BEP flow or just for short periods in a day of the lowest and highest consumption.

Table 2. Effects of PAT's operation limits on the optimal BEPs for three PRV case studies

	Site 13			Site 28			Site 1		
P_{rel}^{max} [-]	1	1.5	2	1	1.5	2	1	1.5	2
Q_{max} [l s^{-1}]	37.74	39.35	41.87	121.99	130.82	139.07	278.82	293.86	323.77
Q_{BEP} [l s^{-1}]	37.74	33.25	31.20	121.99	111.98	105.67	278.82	250.63	244.70
H_{BEP} [m]	75.82	62.21	57.79	64.05	55.34	52.30	55.68	46.39	44.69
n [rpm]	3020	3020	3020	3020	3020	3020	1510	1510	1510
Ns [rpm (m^3 s^{-1})$^{0.5}$ m$^{-0.75}$]	22.83	24.86	25.45	46.59	49.81	50.48	39.12	42.53	43.21
η_{max} [-]	0.77	0.77	0.77	0.83	0.83	0.83	0.85	0.85	0.85
P_{BEP} [kW]	21.58	15.65	13.63	63.81	50.41	44.86	129.29	96.68	90.89
η_{global} [-]	0.61	0.62	0.60	0.65	0.66	0.65	0.67	0.66	0.65
E [MWh year^{-1}]	143.35	143.81	140.61	414.25	416.51	411.26	876.29	874.15	855.95
NPV_{10} [€ year^{-1}]	70284	77854	78134	217052	233338	235555	456731	493662	497327
PP [years]	1.67	1.36	1.29	1.42	1.20	1.12	1.43	1.16	1.11
Q_{BEP}/Q_{ave} [-]	1.04	0.92	0.86	1.02	0.93	0.88	1.01	0.91	0.89
H_{BEP}/H_{ave} [-]	1.00	0.82	0.76	1.03	0.89	0.84	1.00	0.83	0.80
Optimal commercial family	65-200, n=3020, D=219	50-160, n=3020, D=174	50-160, n=3020, D=174	150-500-1, n=1005, D=500	100-160, n=3020, D=185	125-315, n=1510, D=334	300-500, n=1005, D=520	200-330, n=1510, D=330	200-330, n=1510, D=330

The aim of this subsection was to investigate the influence of different HR limits, primarily the maximal flow on the final location of the optimal BEP and the maximization of energy recovery. Three alternatives were examined. The maximal flow was set to correspond the relative mechanical power, $P_{rel}(Q_{max})$, of 1 (i.e., Q_{BEP}), 1.5 and 2. The minimal flows were set with the same principal explained in the methodology section resulting in $P_{rel}(Q_{min})$ of 0.25, 0.375 and 0.5. The results of the analysis for all three sites are presented in Tab. 2. The graphical interpretation of the results for Site 13, is also presented in Fig. 10 and Fig. 2. Fig. 10 presents the results for the first and third alternative of the upper operational limit, while the second alternative is presented in Fig. 2. As it can be seen in Tab. 2, the optimal BEPs were indeed close to the average points when $Q_{max} = Q_{BEP}$, for all three sites. On the other hand, for the 2nd and 3rd alternative of the upper operational limit the optimal BEP flow was 10.3% and 14.6% smaller than this value, on average, respectively. Similarly, on average, the optimal BEP head for the 2nd and 3rd alternative was 16.2% and 20.8% smaller than the optimal BEP head obtained for the 1st alternative of the upper operational limit. For Site 13, Fig. 10 gives an additional insight and that is that for the 3rd alternative the maximal flow through the PAT was never reached, meaning the two CVs were never active at the same time (there are not black crosses), unlike in the first two alternatives.

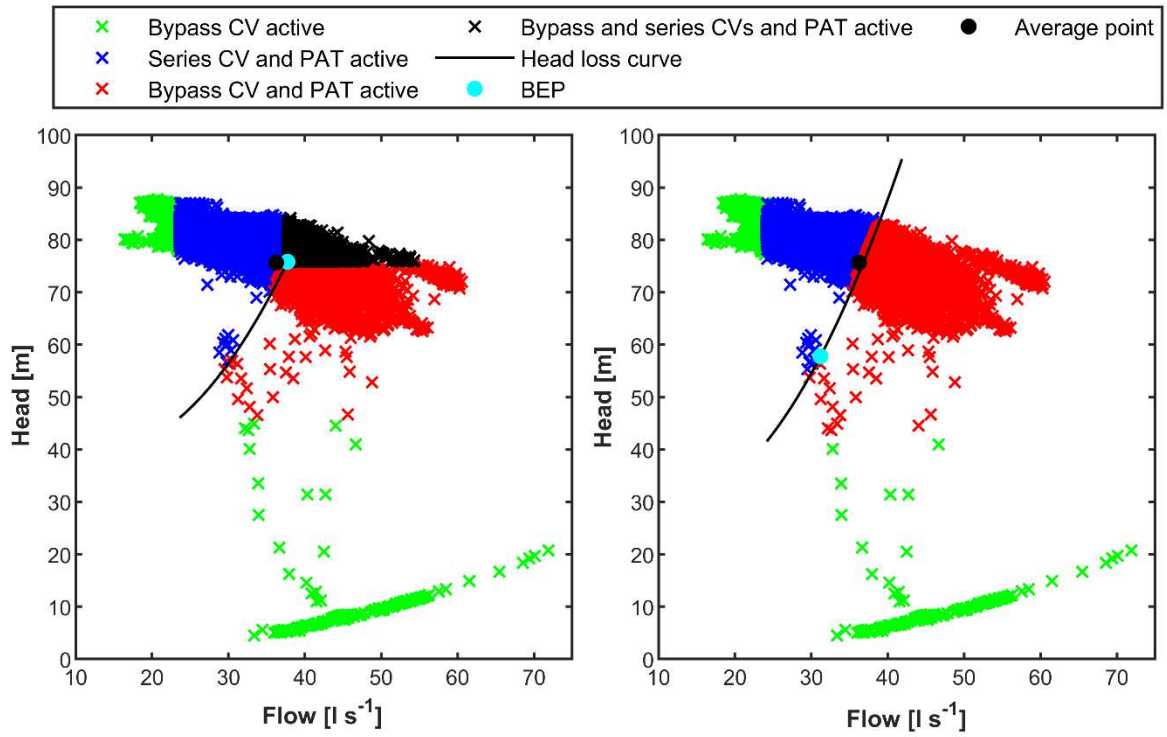

Fig. 10. Influence of PAT's operation limits on the optimal BEP a) $P_{rel}(Q_{max})$ = 1 b) $P_{rel}(Q_{max})$ = 2.

The results in Tab. 2 also suggest that the increase of the maximal flow does not always increase the energy recovery. This suggests that the maximal permissible flow should also be a design variable. Finally, the last row of Tab. 2 suggests that similarly to the effect of different objectives, different selection of the upper operational limit can also result in the selection of different commercial families.

As it was mentioned previously a detailed load analysis should determine that the maximal permissible flow does not exceed the values of the maximal permissible torque and its operation is safe in respect to cavitation occurrence.

4.4 Benchmarks

Finally, the proposed methodology was applied to real-world sites previously used in the literature for comparison. All the results in this subsection were obtained by maximizing the energy recovery objective, i.e., the global plant efficiency, as this was the objective used in the compared studies.

Tab. 3 presents the results obtained by applying the proposed methodology to the sites from Carravetta et al. (2012). The results showed improvements in terms of the global efficiency of the plant ranging from 4.9% to 9.4% depending on the site. The improvements gained were the result of the different restrictions to the solution space of the BEP and sligtly higher predicted η_{max} comparing to the η_{max} of the prototype used in the study. As it can be seen in Tab. 3 the impeller diameters and even rotational speed of the most suitable PATs available on the market can differ from the ones obtained using the affinity laws.

Regardless of the improvements obtained in comparison to the results obtained by Carravetta et al. (2012), the similarity curves extrapolated from the prototype data intersected the operating points of the considered sites. Meaning that the appropriate PAT model for the considered sites should be hydraulically similar to the prototype (i.e., have similar value of N_s). Tab. 4, which presents the results of comparison with Lydon et al. (2017), indicates that the improvements can be significantly higher if a non-optimal prototype is selected. The improvements gained in terms of η_{global} ranged from 24% to 36% comparing to design points and from 45% to 58% comparing to BEPs of machines similar to prototype. The improvements of this magnitude, especially in case of the machines similar to prototype, can be explained with the efficiency of the prototype which was around 20% lower than the predicted values and the fact that the prototype's affinity curve for n = 900 rpm was very far away from the operating points of all three considered sites. Although the PRV sites are the same it has to be pointed out that the measurements have not been recorded for the same year. However the gross powers of the sites presented in the study were similar.

Table 3. Comparison of the results with methodology proposed in Carravetta et al. (2012)

	Site A1		Site A2		Site A3	
Methodology	Carravetta et al. (2012)	Proposed methodology	Carravetta et al. (2012)	Proposed methodology	Carravetta et al. (2012)	Proposed methodology
Q_{BEP} [l s^{-1}]	30.63	23.94	25.19	23.55	25.73	22.57
H_{BEP} [m]	72.14	55.11	25.12	26.14	14.84	16.46
n [rpm]	3000	3020	1500	1510	1000	1510
Ns [rpm (m^3 s^{-1})$^{0.5}$ m$^{-0.75}$]	21.21	23.10	21.21	20.04	21.21	27.75
η_{max} [-]	0.71	0.75	0.71	0.74	0.71	0.76
P_{BEP} [kW]	15.39	9.72	4.41	4.44	2.66	2.78
η_{global} [-]	0.57	0.63	0.54	0.59	0.49	0.58
η_{global}/η_{max} [-]		0.84		0.80		0.77
E [MWh year^{-1}]	70.57	77.76	33.31	36.31	20.08	23.95
NPV_{10} [€ year^{-1}]	n/a	40934	n/a	15353	n/a	8168
PP [years]	n/a	1.87	n/a	3.02	n/a	3.93
Model	D=194 similar to prototype	40-160, n=3020, η_{global}=0.51	D=229 similar to prototype	65-200, n=1510, η_{global}=0.58	D=264 similar to prototype	65-160, n=1510, η_{global}=0.55

As it was indicated by the results in Tables 3 and 4, the non-optimal choice of the prototype and its speed can seriously dimish the results of the energy recovery. Selection of the prototype, i.e., the specific speed which is a good fit for a site within WDNs which are characterized with large variations

of flow and head is not straighforward. Additionally the characteristic curves of the such prototype could be unavailable. The main advantage of the proposed methodology is that it does not depend on the choice of the prototype and that it will always provide the upper bound of the energy recovery for the examined site.

Table 4. Comparison of the results with methodology proposed by Lydon et al. (2017)

Methodology	BHB (Site 1)			Poplar (Site 13)			Rialto (Site 28)		
	Lydon et al. (2017) Design point)	Lydon et al. (2017) (Similar to protoype)	Proposed methodology	Lydon et al. (2017) Design point)	Lydon et al. (2017) (Similar to protoype)	Proposed methodology	Lydon et al. (2017) Design point)	Lydon et al. (2017) (Similar to protoype)	Proposed methodology
Q_{BEP} [l s^{-1}]	168.00	158.00	250.64	27.00	27.00	33.25	97.00	110.00	111.98
H_{BEP} [m]	69.00	37.00	46.39	95.00	12.00	62.21	76.00	30.00	55.34
n [rpm]	n/a	900	1510	n/a	900	3020	n/a	900	3020
Ns [rpm (m^3 s^{-1})$^{0.5}$ m$^{-0.75}$]	n/a	23.85	42.51	n/a	22.94	24.86	n/a	23.29	49.81
η_{max} [-]	0.62	0.62	0.85	0.62	0.62	0.77	0.62	0.62	0.83
P_{BEP} [kW]	70.50	35.56	96.76	15.60	1.97	15.65	44.84	20.07	50.41
η_{global} [-]	0.30	0.21	0.66	0.35	0.04	0.62	0.42	0.15	0.66
η_{global}/η_{max} [-]			0.78			0.80			0.79
E [MWh year^{-1}]	392.91	274.50	874.15	101.12	11.41	143.81	345.38	123.03	416.51
NPV_{10} [€ year^{-1}]	n/a	n/a	493662	n/a	n/a	77854	n/a	n/a	233338
PP [years]	n/a	n/a	1.16	n/a	n/a	1.36	n/a	n/a	1.20
Model	n/a	D=450mm, similar to prototype	200-330, n=1510, η_{global}=0.66	n/a	D=250mm, similar to prototype	50-160, n=3020, η_{global}=0.61	n/a	D=400mm, similar to prototype	100-160, n=3020, η_{global}=0.65

Some of the previous studies suggested η_{global} = 0.6 as maximal global efficiency of a hydro plant within a WDN equiped with a PAT (Carravetta et al., 2014; Fecarotta et al., 2018). The results of the six examined sites presented in Tab. 3 and 4 provide a different definition of the upper bound of the energy recovery using hydraulic regulation. The results suggest that the maximal global efficiency of a plant is around 80% of the η_{max} of the optimal PAT.

5 Conclusions

This paper presents a novel methodology for the selection of a PAT from the market to replace a PRV located within WDNs, which are characterized by large flow and head fluctuations. The presented methodology implements the classical hydraulic regulation scheme with two control valves and a single-stage centrifugal PAT for maintenance of required downstream head pattern. It also employs the NMSDS optimization algorithm to find the optimal BEP. Besides the optimization algorithm used, the approach in this paper differs from previous approaches in restriction of the solution space. Unlike traditional approaches which are based on scaling a prototype data by affinity curves and thus restricting the solution space to these curves, the proposed methodology restricts the solutions space only with the availability boundaries of market centrifugal PATs.

Using the proposed methodology, this study examined the effects of different objectives, namely maximization of energy recovery, maximization of NPV_{10} and minimization of PP on the selection of the optimal PAT. The results of three real world PRV case studies from Dublin WDN showed that the optimal BEPs for the three objectives correspond to 92%, 87% and 64% of the sites' average operating flow and 85%, 78% and 75% of the sites' average operating head, on average across three sites,

respectively. The results also showed that the former differences in the theoretically optimal BEPs can result in selection of different commercial pump families. Although the selection of commercial families should be regarded with caution as the validation section of this paper indicated that even the most accurate models for predicting the BEP in turbine mode can result in errors of around 30%.

This paper also suggested new formulation for the limits of variable PAT operation based on its relative mechanical power (P_{rel}). Varying the upper operational limit the paper investigated how it can affect the selection of the optimal PAT and the maximization of energy recovery. The results of the same three PRV case studies showed that the increase of the maximal permissible flow results in a theoretically smaller PAT but it does not always increase the maximal value of the energy recovery. Similarly to the effect of the selection of different objectives the results showed that the selection of different upper operational limit can also result in selection of different commercial pump family. This indicates that the upper operation limit should also be one of the designed variables.

The methodology was also applied to sites previously used in the literature resulting in improvements in terms of the global plant's efficiency of 4.9% to 9.4% comparing with Carravetta et al. (2012) and 24% to 58% comparing to Lydon et al. (2017). The results of the maximal global efficiency for the six sites from these 2 studies suggest that the upper bound of the energy recovery is around 80% of the η_{max} of the optimal PAT.

The future work will be focused on studying the flow and head patterns of the PRV database in order to find out what are the minimal flow and head characteristics of a PRV which would result in economically viable replacement.

6 Data Availability Statements

Some or all data, models, or code used during the study were provided by a third party. These are: Flow and head recordings at case study valves. Direct request for these materials may be made to the provider as indicated in the Acknowledgments.

Some or all data, models, or code that support the findings of this study are available from the corresponding author upon reasonable request. These are: MATLAB code used for the analysis in the presented paper; Pump characteristic curves booklets used to define the availability boundaries (KSB, 2018).

7 Acknowledgments

This investigation was part funded by the European Regional Development Funds, Interreg Atlantic Area Programme 2014-2020, through the REDAWN project (EAPA 198_2016).

The authors would also like to thank Dublin City Council and Seville Water Supply Company (EMASESA) for providing the recordings at their pressure reducing valves.

8 Notation

The following symbols are used in this paper:

H = hydraulic head [m]

N = number of the operating points, i.e., time steps [-]

NPV_{10} = net present value after 10 years [€]

N_s = specific speed based on unit flow [rpm $(m^3\ s^{-1})^{0.5}(m)^{-0.75}$]

OMC – operation and management costs [€]

P = power generated by the PAT [kW]

PP = payback period of investment [years]

P_{rel} = relative power generated by the PAT [-]

Q = flow rate [l s^{-1}]

R^2 = coefficient of determination [-]

R^4 = accuracy metric created by multiplying R2 of head loss and power curves [-]

TIC = total installation costs [€]

a, b, c, d, e, f – polynomial coefficients of the PAT characteristic curves defined by Novara and McNabola (2018)

e_{up} = electricity unit price [€ MWh^{-1}]

g = gravitational acceleration [m s^{-2}]

n = rotational speed of impeller [rpm]

pp = number of magnetic pole pairs [-]

r = discount rate [-]

$\mathbf{x}_1$ = the best point in the simplex

$\mathbf{x}_{k+1}$ = the worst point in the simplex

$\mathbf{x}_m$ = centroid of the simplex points excluding the best

Δt– time step duration [h]

η = PAT's efficiency [-]

ρ = water density [kg m^{-3}]

9 Supplemental Materials

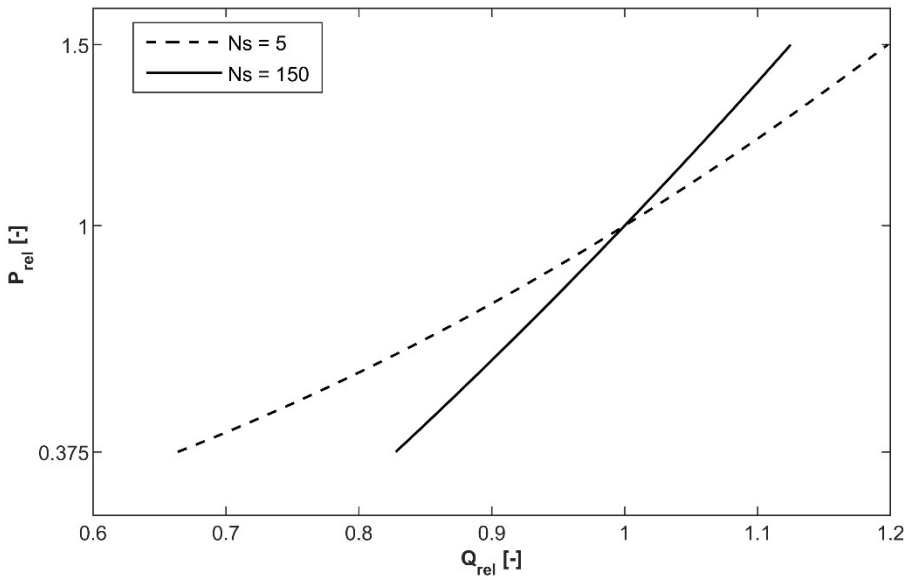

Fig. S1. Steepness of relative power curves as a function of N_s

Tab. S1. Five commercial pump families with the highest values of energy recovery for Site 13.

Family	50-160	65-315	65-200	50-315	40-160
D [mm]	174	320	219	323	174
Q_{BEP} [l s^{-1}]	34.32	34.20	47.05	23.62	19.12
H_{BEP} [m]	59.03	60.39	96.79	66.82	67.76
n [rpm]	3020	1510	3020	1510	3020
Ns [rpm (m^3 s^{-1})$^{0.5}$ m$^{-0.75}$]	26.27	12.89	21.23	9.93	17.68
η_{max} [-]	0.78	0.69	0.77	0.62	0.71
P_{BEP} [kW]	15.44	13.90	34.37	9.57	9.02
η_{global} [-]	0.61	0.55	0.49	0.42	0.40
E [MWh year^{-1}]	141.63	127.99	114.36	99.14	94.20
NPV_{10} [€ year^{-1}]	76247	66836	45426	51413	49625
PP [years]	1.39	1.53	2.64	1.56	1.49

Tab. S2. Five commercial pump families with the highest values of energy recovery for Site 28.

Family	100-160	125-315	150-500-1	80-160	100-200
D [mm]	185	334	500	174	219
Q_{BEP} [l s^{-1}]	110.92	109.16	109.44	84.39	112.75
H_{BEP} [m]	51.70	53.00	56.61	44.29	85.28
n [rpm]	3020	1510	1005	3020	3020
Ns [rpm (m^3 s^{-1})$^{0.5}$ m$^{-0.75}$]	52.16	25.40	16.11	51.10	36.14
η_{max} [-]	0.83	0.81	0.76	0.82	0.83
P_{BEP} [kW]	46.56	45.99	46.14	30.11	78.22
η_{global} [-]	0.65	0.65	0.61	0.57	0.52
E [MWh year^{-1}]	415.14	412.36	386.54	362.22	332.38
NPV_{10} [€ year^{-1}]	234498	230800	197782	211786	162454
PP [years]	1.15	1.20	1.63	0.98	1.83

Tab. S3. Five commercial pump families with the highest values of energy recovery for Site 1.

Family	200-330	250-500	300-500	250-400	200-400
D [mm]	330	520	520	405	405
Q_{BEP} [l s^{-1}]	248.81	261.53	309.05	349.96	241.70
H_{BEP} [m]	42.47	51.31	55.15	67.16	72.86
n [rpm]	1510	1005	1005	1510	1510
Ns [rpm (m^3 s^{-1})$^{0.5}$ m$^{-0.75}$]	45.27	26.81	27.61	38.07	29.77
η_{max} [-]	0.85	0.83	0.84	0.85	0.84
P_{BEP} [kW]	87.83	109.56	139.96	196.50	144.68
η_{global} [-]	0.66	0.66	0.62	0.55	0.53
E [MWh year^{-1}]	867.54	865.59	813.96	728.28	700.07
NPV_{10} [€ year^{-1}]	494511	447698	378465	318395	350014
PP [years]	1.11	1.58	2.04	2.29	1.73

10 References

Alatorre-Frenk, C., 1994. Cost Minimisation in Micro-Hydro Systems Using Pumps-As-Turbines. University of Warwick.

Araujo, L.S., Ramos, H., Coelho, S.T., 2006. "Pressure Control for Leakage Minimisation in Water Distribution Systems Management". *Water Resour. Manag.* 20, 133–149. https://doi.org/10.1007/s11269-006-4635-3

Barbarelli, S., Amelio, M., Florio, G., 2017a. "Experimental activity at test rig validating correlations to select pumps running as turbines in microhydro plants". *Energy Convers. Manag.* 149, 781–797. https://doi.org/10.1016/j.enconman.2017.03.013

Barbarelli, S., Amelio, M., Florio, G., Scornaienchi, N.M., 2017b. "Procedure Selecting Pumps Running as Turbines in Micro Hydro Plants". *Energy Procedia* 126, 549–556. https://doi.org/10.1016/j.egypro.2017.08.282

Bozorgi, A., Javidpour, E., Riasi, A., Nourbakhsh, A., 2013. "Numerical and experimental study of using axial pump as turbine in Pico hydropower plants". *Renew. Energy* 53, 258–264. https://doi.org/10.1016/j.renene.2012.11.016

Calado, T.V.R., 2014. Micro-produção de energia: caso de Loures. Universidade de Lisboa.

Carravetta, A., del Giudice, G., Fecarotta, O., Ramos, H.M., 2013. "PAT design strategy for energy recovery in water distribution networks by electrical regulation". *Energies* 6, 411–424. https://doi.org/10.3390/en6010411

Carravetta, A., Del Giudice, G., Fecarotta, O., Ramos, H.M., 2012. "Energy Production in Water Distribution Networks: A PAT Design Strategy". *Water Resour. Manag.* 26, 3947–3959. https://doi.org/10.1007/s11269-012-0114-1

Carravetta, A., Fecarotta, O., Del Giudic, G., Ramos, H., 2014. "Energy recovery in water systems by PATs: A comparisons among the different installation schemes". *Procedia Eng.* 70, 275–284. https://doi.org/10.1016/j.proeng.2014.02.031

Carravetta, A., Houreh, S.D., Ramos, H.M., 2018. Pump as Turbines Fundamentals and Applications. Springer, Cham, Switzerland. https://doi.org/10.1007/978-3-662-48465-4

Chapallaz, J., Eichenberg, P., Fisher, G., 1992. Manual on Pumps Used as Turbines, Manual on pumps used as turbines. (GTZ) GmbH, Germany.

Coelho, B., Andrade-Campos, A.A., 2018. "Energy recovery in water networks: Numerical decision support tool for optimal site and selection of micro turbines". *J. Water Resour. Plan. Manag.* 144, 04018004. https://doi.org/10.1061/(ASCE)WR.1943-5452.0000894

Colombo, A., Kleiner, Y., 2011. "Energy recovery in water distribution systems using microturbines". *Probabilistic Methodol. water wastewater Eng. (in honour Prof. Barry Adams, Univ. Toronto)* 1–9.

Corcoran, L., Coughlan, P., Mc Nabola, A., 2013. "Energy recovery potential using micro hydropower in water supply networks in the UK and Ireland". *Water Sci. Technol. Water Supply* 13, 552–560. https://doi.org/10.2166/ws.2013.050

Corcoran, L., McNabola, A., Coughlan, P., 2016. "Optimization of water distribution networks for combined hydropower energy recovery and leakage reduction". *J. Water Resour. Plan. Manag.* 142, 1–8. https://doi.org/10.1061/(ASCE)WR.1943-5452.0000566

Delgado, J., Ferreira, J.P., Covas, D.I.C., Avellan, F., 2019. "Variable speed operation of centrifugal

pumps running as turbines. Experimental investigation". *Renew. Energy* 142, 437–450. https://doi.org/10.1016/j.renene.2019.04.067

Deprez, W., Dexters, A., Driesen, J., Belmans, R., 2006. "Energy efficiency of small induction Machines: Comparison between Motor and Generator Mode", in: In Proceedings of ICEM 2006: XVII International Conference on Electrical Machines. IEEE, p. 6.

Derakhshan, S., Nourbakhsh, A., 2008. "Experimental study of characteristic curves of centrifugal pumps working as turbines in different specific speeds". *Exp. Therm. Fluid Sci.* 32, 800–807. https://doi.org/10.1016/j.expthermflusci.2007.10.004

Electric Ireland, n.d. Electric Ireland Micro-Generation Pilot Scheme [WWW Document]. URL https://www.electricireland.ie/residential/help/efficiency/electric-ireland-micro-generation-pilot-scheme (accessed 4.2.20).

Fecarotta, O., Aricò, C., Carravetta, A., Martino, R., Ramos, H.M., 2014. "Hydropower Potential in Water Distribution Networks: Pressure Control by PATs". *Water Resour. Manag.* 29, 699–714. https://doi.org/10.1007/s11269-014-0836-3

Fecarotta, O., Carravetta, A., Ramos, H.M., Martino, R., 2016. "An improved affinity model to enhance variable operating strategy for pumps used as turbines". *J. Hydraul. Res.* 54, 332–341. https://doi.org/10.1080/00221686.2016.1141804

Fecarotta, O., Mc Nabola, A., 2017. "Optimal Location of Pump as Turbines (PATs) in Water Distribution Networks to Recover Energy and Reduce Leakage". *Water Resour. Manag.* 31, 5043–5059. https://doi.org/10.1007/s11269-017-1795-2

Fecarotta, O., Ramos, H.M., Derakhshan, S., Del Giudice, G., Carravetta, A., 2018. "Fine tuning a PAT hydropower plant in a water supply network to improve system effectiveness". *J. Water Resour. Plan. Manag.* 144, 1–12. https://doi.org/10.1061/(ASCE)WR.1943-5452.0000961

Fernández Garcia, I., Mc Nabola, A., 2020. "Maximizing Hydropower Generation in Gravity Water Distribution Networks: Determining the Optimal Location and Number of Pumps as Turbines". *J. Water Resour. Plan. Manag.* 146, 1–12. https://doi.org/10.1061/(ASCE)WR.1943-5452.0001152

Fernández García, I., Novara, D., Nabola, A.M., 2019. "A model for selecting the most cost-effective pressure control device for more sustainable water supply networks". *Water (Switzerland)* 11. https://doi.org/10.3390/w11061297

Fontana, N., Giugni, M., Glielmo, L., Marini, G., 2016. "Real time control of a prototype for pressure regulation and energy production in water distribution networks". *J. Water Resour. Plan. Manag.* 142. https://doi.org/10.1061/(ASCE)WR.1943-5452.0000651

Gallagher, J., Harris, I.M., Packwood, A.J., McNabola, A., Williams, A.P., 2015. "A strategic assessment of micro-hydropower in the UK and Irish water industry: Identifying technical and economic constraints". *Renew. Energy* 81, 808–815. https://doi.org/10.1016/j.renene.2015.03.078

Gomes, R., Sá Marques, A., Sousa, J., 2012. "Identification of the optimal entry points at District Metered Areas and implementation of pressure management". *Urban Water J.* 9, 365–384. https://doi.org/10.1080/1573062X.2012.682589

KSB, 2018. Etanorm Characteristic Curves Booklets 50 Hz [WWW Document]. URL https://shop.ksb.com/ims_docs/00/00215A9B0E3D1EEABB91CFF769126DF9.pdf (accessed 10.6.20).

Lagarias, J.C., Reeds, J.A., Wright, M.H., Wright, P.E., 1998. "Convergence properties of the Nelder--Mead simplex method in low dimensions". *SIAM J. Optim.* 9, 112–147.

https://doi.org/10.1137/S1052623496303470

Lima, G.M., Luvizotto, E., Brentan, B.M., 2017. "Selection and location of Pumps as Turbines substituting pressure reducing valves". *Renew. Energy* 109, 392–405. https://doi.org/10.1016/j.renene.2017.03.056

Lydon, T., Coughlan, P., McNabola, A., Mc Nabola, A., 2017. "Pressure management and energy recovery in water distribution networks: Development of design and selection methodologies using three pump-as-turbine case studies". *Renew. Energy* 114, 1038–1050. https://doi.org/10.1016/j.renene.2017.07.120

McNabola, A., Coughlan, P., Corcoran, L., Power, C., Williams, A.P., Harris, I., Gallagher, J., Styles, D., 2014. "Energy recovery in the water industry using micro-hydropower: An opportunity to improve sustainability". *Water Policy* 16, 168–183. https://doi.org/10.2166/wp.2013.164

Novara, D., 2020. Hydropower Energy Recovery Systems: Development of Design Methodologies for Pumps As Turbines in Water Networks. University of Dublin, Trinity College Dublin.

Novara, D., Carravetta, A., McNabola, A., Ramos, H.M., Mc Nabola, A., Ramos, H.M., 2019. "Cost Model for Pumps as Turbines in Run-of-River and In-Pipe Microhydropower Applications". *J. Water Resour. Plan. Manag.* 145, 04019012. https://doi.org/10.1061/(ASCE)WR.1943-5452.0001063

Novara, D., Derakhshan, S., McNabola, A., Ramos, H., 2017. "Estimation of unit cost and maximum efficiency for Pumps as Turbines", in: Young Water Professionals. IWA, Budapest.

Novara, D., Mc Nabola, A., 2018. "The Development of a Decision Support Software for the Design of Micro-Hydropower Schemes Utilizing a Pump as Turbine". *Proceedings* 2, 678. https://doi.org/10.3390/proceedings2110678

Novara, D., McNabola, A., 2018. "A model for the extrapolation of the characteristic curves of Pumps as Turbines from a datum Best Efficiency Point". *Energy Convers. Manag.* 174, 1–7. https://doi.org/10.1016/j.enconman.2018.07.091

Pugliese, F., De Paola, F., Fontana, N., Giugni, M., Marini, G., 2016. "Experimental characterization of two Pumps As Turbines for hydropower generation". *Renew. Energy* 99, 180–187. https://doi.org/10.1016/J.RENENE.2016.06.051

Sebastião, A.F.F., 2017. A platform for assessment of energy recovery technologies by pressure reduction in water distribution networks. NOVA Univeristy of Lisbon.

Sinagra, M., Sammartano, V., Morreale, G., Tucciarelli, T., 2017. "A new device for pressure control and energy recovery in water distribution networks". *Water (Switzerland)* 9, 1–14. https://doi.org/10.3390/w9050309

Stefanizzi, M., Capurso, T., Balacco, G., Torresi, M., Binetti, M., Piccinni, A.F., Fortunato, B., Camporeale, S.M., 2018. "Preliminary assessment of a pump used as turbine in a water distribution network for the recovery of throttling energy", in: Proceedings of 12th European Conference on Turbomachinery Fluid Dynamics & Thermodynamics. Lausanne, Switzerland.

Stepanoff, A.J., 1957. Centrifugal and axial flow pumps: Theory, Design, and Application. Wiley.

Tricarico, C., Morley, M.S., Gargano, R., Kapelan, Z., Savić, D., Santopietro, S., Granata, F., de Marinis, G., 2018. "Optimal energy recovery by means of pumps as turbines (PATs) for improved WDS management". *Water Sci. Technol. Water Supply* 18, 1365–1374. https://doi.org/10.2166/ws.2017.202

Vicente, D.J., Garrote, L., Sánchez, R., Santillán, D., 2016. "Pressure management in water distribution systems: Current status, proposals, and future trends". *J. Water Resour. Plan. Manag.* 142, 1–13.

https://doi.org/10.1061/(asce)wr.1943-5452.0000589

Williams, A.A., 1996. "Pumps as turbines for low cost micro hydro power". *Renew. Energy* 9, 1227–1234. https://doi.org/10.1016/0960-1481(96)88498-9

Yang, S.S., Derakhshan, S., Kong, F.Y., 2012. "Theoretical, numerical and experimental prediction of pump as turbine performance". *Renew. Energy* 48, 507–513. https://doi.org/10.1016/j.renene.2012.06.002